PERGAMON

Control Engineering Practice 7 (1999) 1467–1482

www.elsevier.com/locate/conengprac

Asynchronous measurement and control: a case study on motor synchronization

W.P.M.H. Heemels[a,*], R.J.A. Gorter[b], A. van Zijl[a], P.P.J. van den Bosch[a], S. Weiland[a], W.H.A. Hendrix[a], M.R. Vonder[c]

[a]*Department of Electrical Engineering, Eindhoven University of Technology, P.O. Box 513, 5600 MB Eindhoven, The Netherlands*
[b]*TNO Industrie, Product development division, P.O. Box 6235, 5600 HE Eindhoven, The Netherlands*
[c]*B.V. Buhrs-Zaandam, P.O. Box 92, 1500 EB Zaandam, The Netherlands*

Received 23 June 1998; accepted 24 June 1999

Abstract

The synchronization between two electrical motors (master and slave) is studied. To reduce the costs of the master–slave combination, the slave motor is mounted with a very low-resolution encoder (one pulse per revolution). Since the position measurements are asynchronous in time, standard control and analysis techniques are not applicable. Two methods are proposed to deal with these cheap, low-resolution encoders: the hybrid and the asynchronous control scheme. The presented controllers are successfully tested on a real industrial master-multi-slave system as is used for mailing machines. © *1999 Elsevier Science Ltd. All rights reserved.*

Keywords: Master–slave system; Synchronization; Encoders; Motor control; Industrial production systems; Discrete event dynamic systems

1. Introduction

In industrial manufacturing systems one often encounters situations in which the position of several electrical motors (slaves) should follow the position of a master motor. Examples are product handling machines and multi-conveyor-belt-systems. Traditionally, this kind of synchronization is achieved with a single mechanical axis that drives all the tools. Nowadays, these mechanical axes are replaced by one or more 'electrical axes' to obtain more flexibility, in the sense that tools can easily be added or removed ('plug-and-play concept'). In case of an electrical axis, a small motor is connected to each tool separately. Automatic control, based on shared signals, is used to synchronize the tools.

In general, the angular position of a driving motor is measured by an encoder, which only gives pulses at fixed positions of the motor axis. Hence, the times at which information about the motor axis position becomes available are not equally spaced in time. Encoders usually have a high resolution, typically from 1000 to 5000 individual measured positions (pulses) per revolution of the motor axis. In practice, high-resolution encoders are read out after fixed time intervals and the discrete-event character of the encoder is neglected.

The company Buhrs–Zaandam B.V. in Zaandam (The Netherlands) builds mailing systems that automatically compose mailings consisting of several brochures. A mailing system is depicted in Fig. 1. The main component of the mailing (e.g. book or magazine) enters the conveyor belt (lug chain) at the loader module (1 in Fig. 1). Several supplements are added to the main product by a feeder module consisting of sheet-feeders 2. Sheet-feeders basically grip a brochure from a stack and put it on the conveyor belt (the master in this case). The main product, together with the supplements, form a package that is wrapped in plastic foil by a packaging module 3. The foil is being supplied by a reel stand 4. Incorrect packages are removed at the rejection module 5. Finally, the product is released after which an address is printed on it, using a label or directly, via an inkjet printer 6. After this the product is put on a stack 7. For such a mailing system it is clear that synchronization is

* Corresponding author. Tel.: +31-40-247-3587; fax: +31-40-243-4582.

E-mail address: w.p.m.h.heemels@tue.nl (W.P.M.H. Heemels)

PII: S0967-0661(99)00113-6

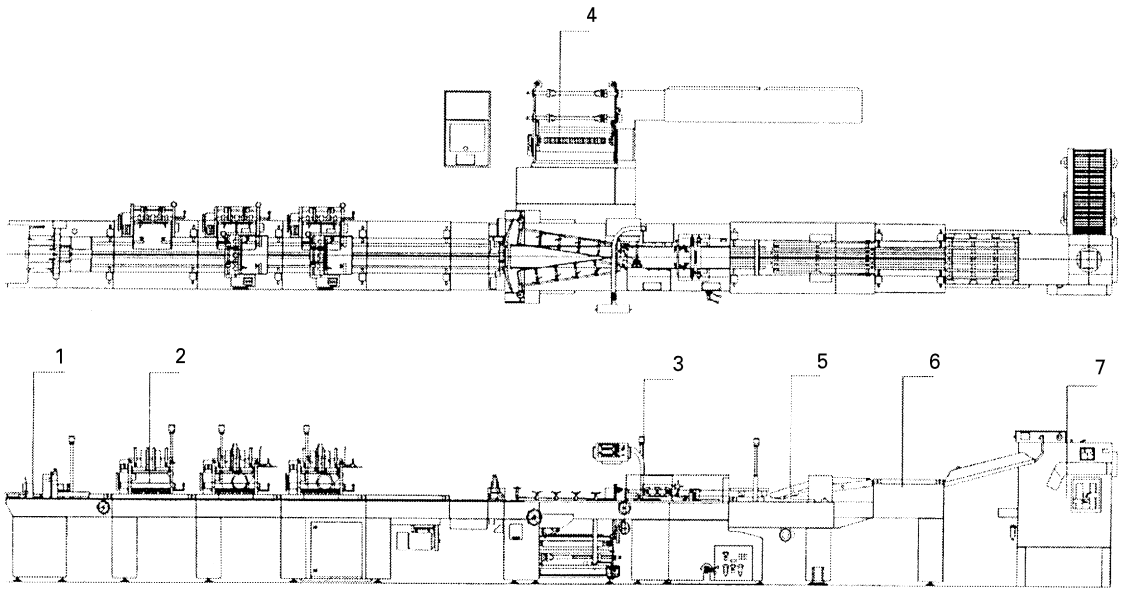

Fig. 1. Mailing system.

required between one master (the conveyor belt) and many slaves.

To reduce the total costs of a mailing system, Buhrs–Zaandam would like to replace the expensive high-resolution encoders of the slaves with cheap low-resolution encoders (with 1–8 measurements per revolution of the motor axis) without losing the tight synchronization between the conveyor belt and the sheet-feeders. With these low resolutions it is no longer possible to neglect the discrete-event character of the sensors.

Indeed, in the motor/encoder combination, measurements are not available at fixed time instants, but at fixed "positions". Other examples of asynchronous sensors include level sensors for measuring the height of a fluid in a tank, (magnetic/optic) disk drives with similar measurement devices and transportation systems where the position is only known when certain markers are passed (De Bruin & van den Bosch, 1998). The literature on sampled-data systems (see e.g. Bamieh & Pearson, 1992; Chen & Qiu, 1994; Voulgaris, 1994; Sågfors & Toivonen, 1997) is not able to deal with such asynchronous measurement devices, since one usually assumes that the times of the control updates and measurements are known a priori and are equally spaced (synchronous) in time.

In the context of motor control with reasonably low-resolution encoders, Hori, Umeno, Uchida and Konno, (1991) and Chiang (1990) propose a multirate scheme, where the control rate is high enough to prevent long deadtimes in the control action and the read-out rate of the encoder is constant, but much smaller than the control rate to prevent large quantization errors in the estimation of the speed. Both papers do not take the discrete-event character of the sensor into account. Therefore, the results are not applicable for extremely low encoder resolutions.

One approach to the problem that incorporates the discrete-event character is described in Philips and Tomizuka (1995). In that paper a discrete-time controller with a fixed control rate is designed based on a state observer with asynchronous updates. The state observer is based on a time-varying Luenberger observer and uses a model to estimate the state of the system between two measurements. This calls for fast processors, since on-line calculation of matrix exponentials and time-varying Luenberger gains is required at every new measurement. This approach is corrupted when (substantial) disturbances are involved, since the estimation becomes unreliable.

In this paper, two alternative methods for motor synchronization will be proposed that result in simple control structures. Both methods have been tested successfully on an experimental set-up consisting of a master motor and a sheet-feeder with only one measurement pulse per revolution of the slave motor axis.

The outline of the paper is as follows. The introduction of the problem is given in Section 2. Next, the performance is determined for encoders with high resolution for both master and slave as a reference. In Section 4, the advantages of using asynchronous measurements are explained. The new control techniques are treated in Sections 5 and 6. In Section 7 additional tests are carried out and in Section 8 the conclusions are stated.

2. Problem formulation

The test set-up (Fig. 2) consists of two induction motors each driving a different load by means of a gear box

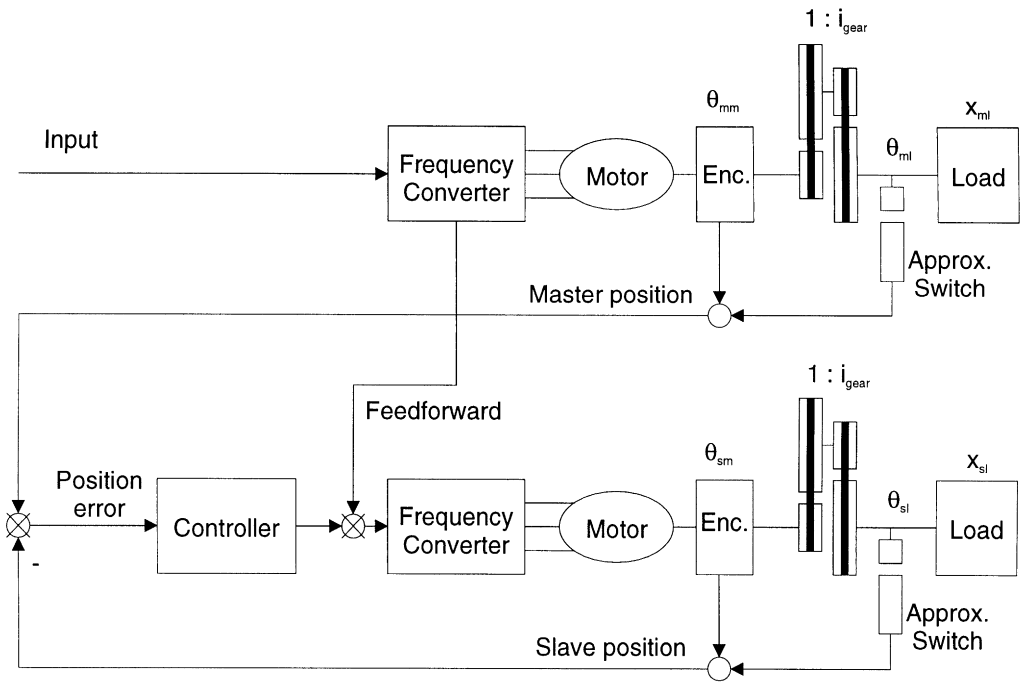

Fig. 2. The test set-up.

(gear ratio i_{gear} is equal to 12.5 meaning that the motor axis turns 12.5 times faster than the load axis). One motor is the master (supposed to drive a conveyor belt) and the other motor is the slave (driving the sheet-feeder). The induction motors are powered by frequency converters (Fig. 2).

As a model for the slave motor and the mechanical system a simple third-order model is used (Leonhard, 1990) given by

$$\dot{\theta}_s(t) = \omega_s(t), \tag{1a}$$

$$\dot{\omega}_s(t) = \frac{1}{J}[T(t) - B\omega_s(t) - d(t)], \tag{1b}$$

$$\dot{T}(t) = \frac{1}{\tau}[-K_t\omega_s(t) - T(t) + K_tK_f\,u(t)], \tag{1c}$$

where θ_s (rad) is the position of the slave motor axis, ω_s (rad/s) the speed of the motor axis, T (N m) the torque generated by the motor, u (V) is the voltage applied to the frequency converter (control input) and d (N m) the torque disturbance generated by the sheet-feeder. In this model the frequency converter is assumed to be linear with a gain K_f (rad/V s). The torque slip-angle curve of the induction motor is linearized by the factor K_t (N m s/rad). J (kg m^2/rad) is the inertia of the rotor plus load and B (N m s/rad) is the mechanical damping. The constant τ (s) represents the electrical time constant in the motor. Using the motor name plate data and various measurements, the model parameters were estimated for the slave motor using techniques of Gorter (1997) resulting in $K_t = 0.35$ N m s/rad, $K_f = 46.3$ rad/V s, $\tau = 0.05$ s, $J = 8.5 \times 10^{-3}$ kg m^2/rad and $B = 9.8 \times 10^{-3}$ N m s/rad.

The slave encoder measures θ_s (rad) with N pulses per revolution of the motor axis. Hence, θ_s is exactly measured only on times t satisfying

$$\theta_s(t) \in \{k\delta_s \mid k \in \mathbb{Z}\}, \tag{2}$$

with $\delta_s := (2\pi/N)$ (rad). The position of the master θ_m will be measured by a high-resolution encoder with 1024 equidistant measurements per revolution yielding a resolution of $\delta_m := 2\pi/1024$. In Fig. 2, $\theta_m = \theta_{mm}$ and $\theta_s = \theta_{sm}$. Furthermore, θ_{ml} (rad) and θ_{sl} (rad) denote the angular position of the load axis of the master and slave, respectively.

The controller must keep the error between master and slave load axis between -0.1 and 0.1 rad. Incorporating the gear ratios gives a maximal allowed error between the position of the motor axes of slave and master of 1.25 rad:

$$\max_{t\geq 0} |\underbrace{\theta_m(t) - \theta_s(t)}_{e_\theta(t)}| \leqslant \varepsilon = 1.25 \text{ rad} \tag{3}$$

irrespective of disturbances and actuator limitations.

The disturbances of the system are mainly due to the varying loads of the motors. In the test set-up a constant load is connected to the master motor. This corresponds to the normal operating conditions of the mailing system, because the load of the conveyor belt is almost constant. The slave drives a so-called sheet-feeder. The sheet-feeder consists of a large metal drum, that is rotated by the motor. To this drum a set of grippers, intended for

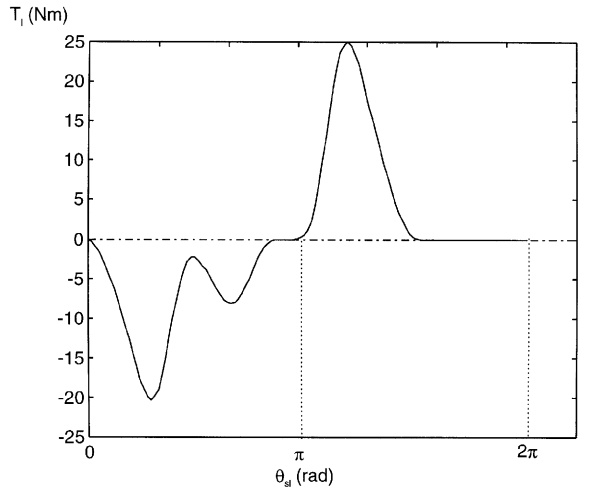

Fig. 3. Sheer-feeder torque (varying part) as function of the load axis position θ_{sl}.

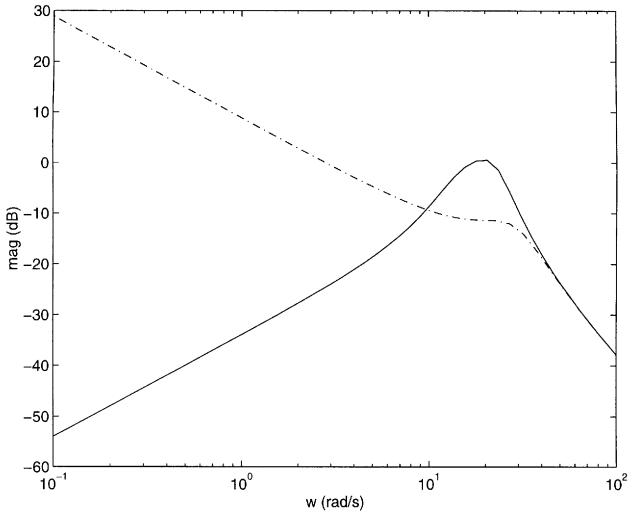

Fig. 4. Bode plot of disturbance rejection (θ_s/d) in controlled (solid) and uncontrolled process (dashed).

grabbing a brochure, is connected. In a mailing system the brochure is transported over the metal drum to a conveyor belt (lug chain), where the brochure is released. The grippers are pressed to the drum by a set of springs. These springs are strained and released via a camshaft attached to the drum. The pressing and releasing of the various springs result in a varying load torque, which has been modelled as a disturbance. As all the operations are cyclic with the rotation of the drum, the torque disturbance that is exerted to the motor depends on the position θ_{sl} (rad) of the load axis (the drum). In Fig. 3 the measured torque as a function of the load axis position θ_{sl} is given. To obtain the torque disturbance d that is exerted on the motor axis, the fluctuating torque of Fig. 3 has to be divided by the gear ratio $i_{gear} = 12.5$, and a constant Coulomb friction torque must be added.

The actuator limitations consist of a saturation and a rate limiter. The input voltage u is limited to the range from 0 to 10 V. Moreover, to bound the slip (the difference between the stator frequency and the mechanical frequency) in the motor, the maximum rate at which u may change is 5 V/s, i.e. $|\dot{u}(t)| \leqslant 5$ V/s for all t.

3. Conventional synchronous control

3.1. Feedforward control part

As a first step in solving the synchronization problem (3), feedforward of the signal coming from the frequency converter of the master to the slave frequency converter is applied (see Fig. 2). In the ideal case when both motors are identical and driving the same load, no additional control action is necessary to keep the motors running synchronously (i.e. $\theta_s(t) = \theta_m(t)$ for all $t \geqslant 0$). In the non-ideal case, θ_s will not be equal to θ_m and a feedback controller is needed to keep the position error bounded as in (3). Since the feed-forward part does not depend on slave and/or master motor positions, it will remain unchanged during all the designs for the feedback controller.

3.2. Feedback control part

As an indication of the achievable performance, a standard PI-controller with a fixed high sample rate is designed on the basis of a high-resolution encoder ($N = 1024$ pulses per revolution) for both the slave and the master motor. The PI-controller has been designed using standard root-locus techniques (see e.g. Franklin, Powell & Naeni, 1994). See Fig. 4 for the closed-loop disturbance rejection (effect of d on θ_s). At low frequencies good disturbance rejection is obtained at the cost of some magnification at frequencies between 10 and 50 rad/s. The rate limiter on the input prevents improvement of the disturbance rejection, even if one uses high-order controllers (Van Zijl, 1997).

To test the controller on the real system, the continuous-time controller was discretized with a sample frequency of 2 kHz (sample time $T_s = 5 \times 10^{-4}$) resulting in the discrete transfer function $H_c(z) = P + I(z-1)^{-1}$ with $P = 0.21$ and $I = 15 \times 10^{-4}$ the proportional and integral constants of the PI-controller. At the sample times both the encoders for slave and master are read out and subtracted from each other to obtain the position error. The choice of sample frequency is a trade-off between a long deadtime for control and a large quantization error caused by the measurement mechanism. The highest relevant process frequency is 20 Hz corresponding to the electrical time constant in (1). A sample frequency of 2 kHz is a reasonable choice, since it is 100 times the highest relevant process frequency and the maximal absolute quantization error is $2\pi/1024 = 6.1 \times 10^{-3}$ rad. To

avoid wind-up of the integrative action, the conditioning technique, as described in Peng, Vrancic and Hanus, 1996 has been used. The pseudo-code for the (feedback) controller can be found in the appendix.

In Fig. 5, the resulting position errors between master and slave are given for different motor speeds.

The position error stays within the required error bound of 1.25 rad. The small fluctuations are caused by the position-dependent disturbance of the sheet-feeder. Since the frequency of this periodic disturbance is directly related to the motor speed, the frequency of the fluctuations differs. Since for the disturbance the first six harmonics are relevant (see Van Zijl, 1997), the frequency band of the disturbance ranges from 1 to 6 times the load speed. The load speed is equal to slave motor speed divided by the gear ratio $i_{gear} = 12.5$. From Fig. 4 it follows that for low motor speeds (42.5 and 138 rad/s), more harmonics fall in the frequency region between 7 and 25 rad/s, where the disturbance attenuation is not as good as for the other frequencies. For high motor speeds (225 and 363 rad/s) the suppression of the disturbance is better resulting in smaller position errors. The fluctuations do not interfere with the correct operation of the mailing machine for any speed. The rate limiter is the bottleneck in achieving a better attenuation of the fluctuations since counteraction of the rapidly varying disturbances requires a high bandwidth of the actuators.

It must be emphasized that expensive encoders are needed for implementing this control scheme. However, as mentioned before, to reduce the costs of the complete mailing machine, the encoder resolution of the slave is lowered from 1024 to N pulses per revolution of the slave motor axis (i.e. $\delta_s = (2\pi/N)$ rad). The same PI-control scheme has been used as for the high encoder case. In Fig. 6, the real experimental position errors are given for $N = 1$. Most striking is that the average value of the

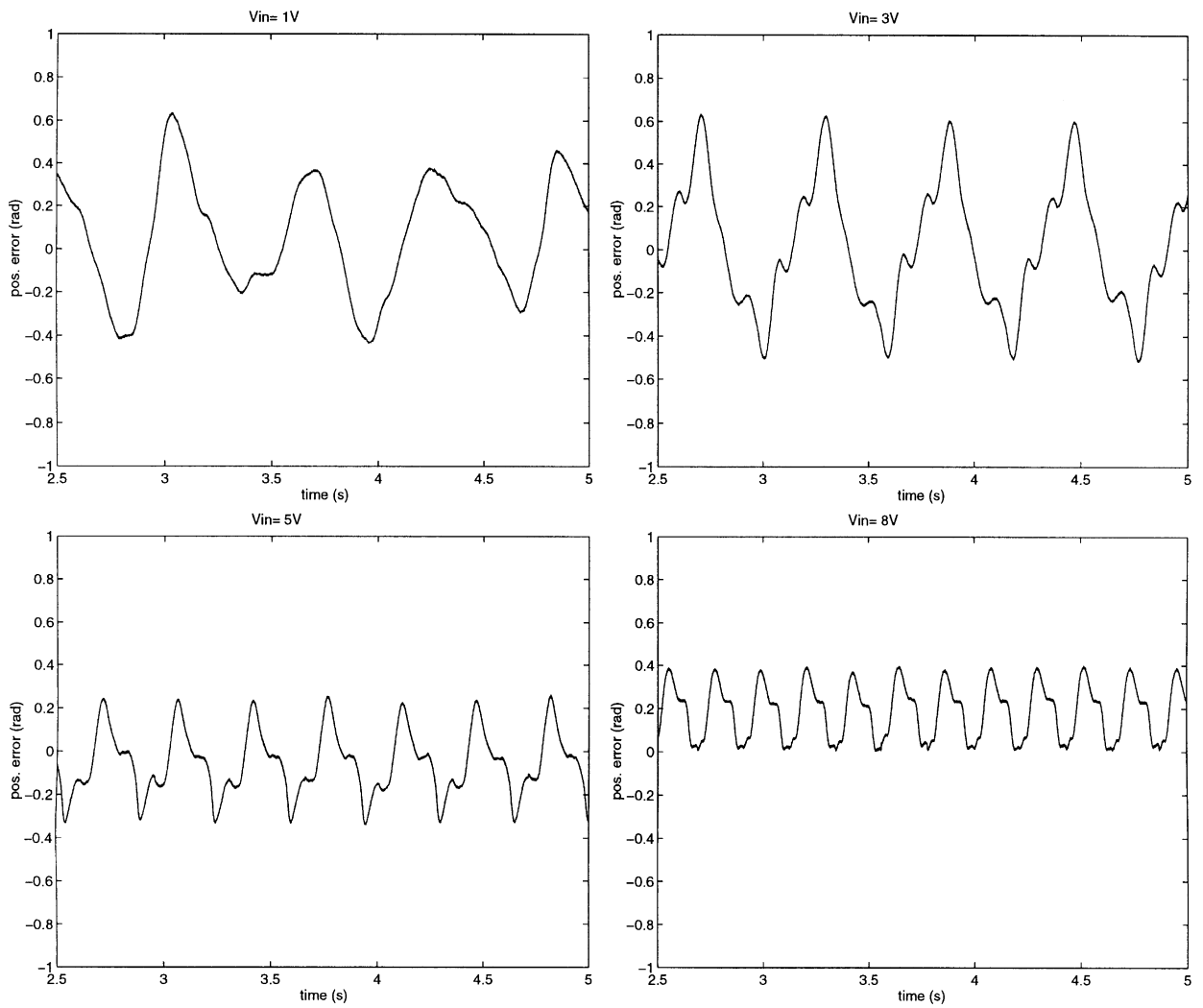

Fig. 5. Position error for different motor speeds (42.5 rad/s) (top left), 138 rad/s (top right), 225 rad/s (bottom left) and 362.5 rad/s (bottom right). The vertical axis reflects the position error in rad and has a range from -1 to 1 rad. On the horizon axis the time is depicted (2.5–5 s).

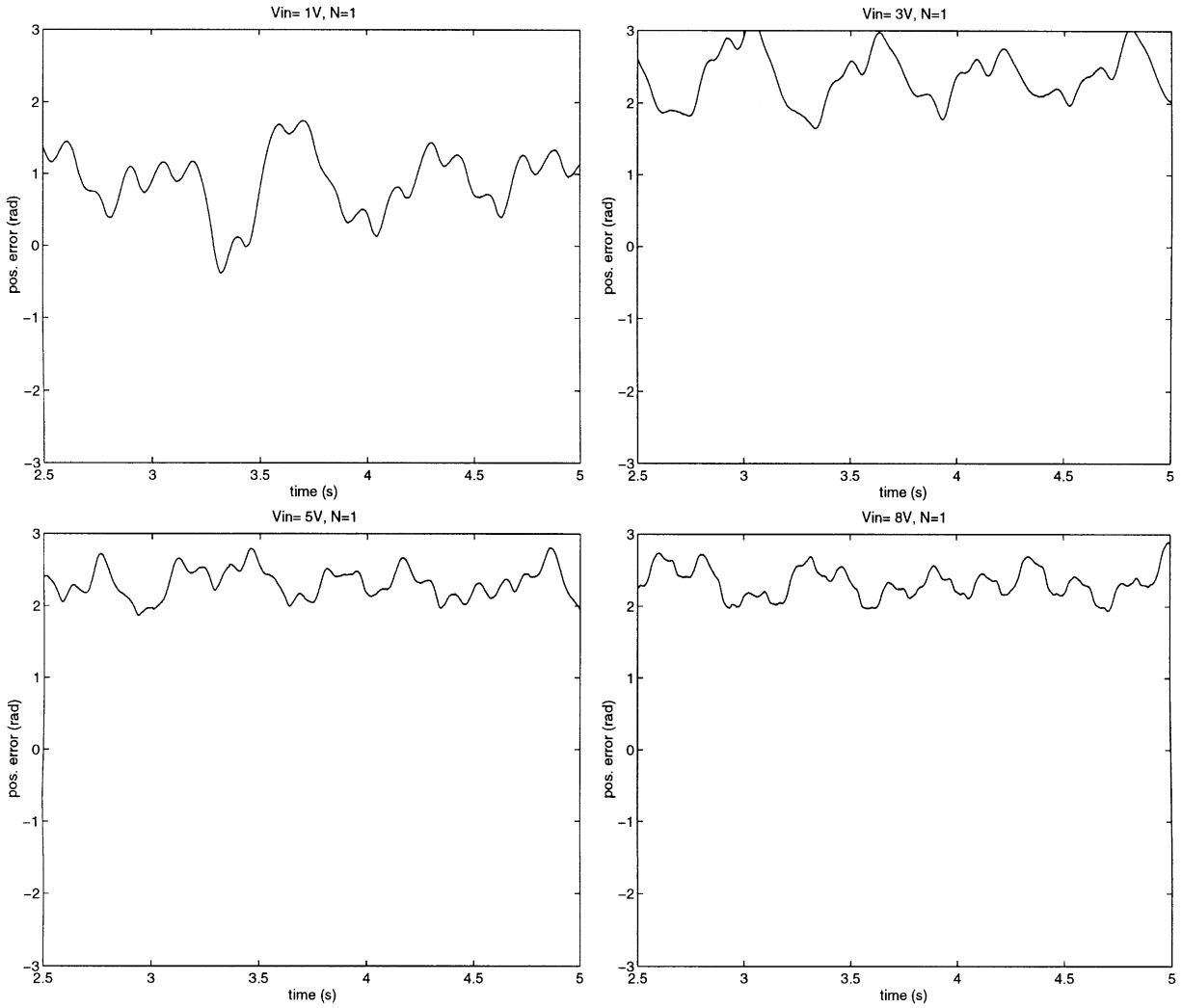

Fig. 6. Position error using one measurement per revolution. The graphs correspond to the same speeds as in Fig. 5. The position error is put at the vertical axis with scale ranging from -3 to 3 rad. The time at the horizontal axis ranges from 2.5 to 5 s.

position error deviates considerably from zero. Furthermore, the fluctuations around the average value of the position error are quite large (up to 2 rad for low speeds) in comparison with the high-resolution case. The control algorithm is based on measured slave positions that will have quantization errors up to $\delta_s = (2\pi/N)$ rad. As a consequence, the 'measured' position error (for an exact definition, see next section) has a mean value of π/N, if the real position error e_θ is identically equal to zero. This explains the non-zero mean of the real position error in Fig. 6. It is obvious that one cannot expect a controller, as implemented above, to meet specifications (3) with such poor measurements.

4. Asynchronous measurements

The first improvement is a better use of the available measurements. The measured signals $\theta_{s,mea}$ for the slave and $\theta_{m,mea}$ for the master are piecewise constant with discontinuities at the time instants that new measurements become available. Formally,

$$\theta_{s,mea}(t) = k\delta_s, \quad \text{if } k\delta_s \leqslant \theta_s(t) < (k+1)\delta_s \tag{4}$$

and similarly,

$$\theta_{m,mea}(t) = k\delta_m, \quad \text{if } k\delta_m \leqslant \theta_m(t) < (k+1)\delta_m\,. \tag{5}$$

From (4) and (5) it follows that

$$0 \leqslant \theta_s(t) - \theta_{s,mea}(t) \leqslant \delta_s\,, \tag{6}$$

$$0 \leqslant \theta_m(t) - \theta_{m,mea}(t) \leqslant \delta_m\,. \tag{7}$$

The measured position error at time t, $e_{\theta,mea}(t) := \theta_{m,mea}(t) - \theta_{s,mea}(t)$ differs from the actual position error $e_\theta(t) = \theta_m(t) - \theta_s(t)$. The difference can be bounded by

$$-\delta_s \leqslant e_\theta(t) - e_{\theta,mea}(t) \leqslant \delta_m. \tag{8}$$

Hence, the difference between the measured and actual position error can increase up to max $(\delta_s, \delta_m) = (2\pi/N)$ rad. However, at times that the slave measurement becomes available, the position error can be determined with an accuracy equal to the high resolution of the master encoder (i.e. $(2\pi/1024)$ rad), since the slave position is exactly known. Denote the collection of these time instants by $\mathscr{D}$, i.e.

$$\mathscr{D} = \{t \geqslant 0 \mid \theta_s(t) = k\delta_s \text{ for some } k \in \mathbb{Z}\}. \tag{9}$$

Since $\theta_{s,mea}(t) = \theta_s(t)$ for all $t \in \mathscr{D}$, it follows from (7) that

$$0 \leqslant e_\theta(t) - e_{\theta,mea}(t) \leqslant \delta_m \quad \text{for all } t \in \mathscr{D}. \tag{10}$$

For times $t \in \mathscr{D}$ the accuracy of the measurement is equal to the master encoder resolution 6.14×10^{-3} rad. It is important to note that this number is independent of the number N of encoder pulses per revolution of the motor axis of the slave. The advantage of a larger N is that more measurements are available in the same time span. Note that the slave position measurements are not distributed equally in time. The method of using the measurements of master and slave position only for times contained in $\mathscr{D}$ is therefore referred to as 'asynchronous measurement'.

5. Hybrid control

A first scheme based on asynchronous measurements is called 'hybrid control'. The controller output is still updated at a fixed rate of 2 kHz resulting in the (controller-) sample times $\{t_i\}_{i \in N}$ with $t_i = iT_s$ s, $i \in \mathbb{N}$ with $T_s = 5 \times 10^{-4}$. The error signal used as input of the PI-controller is kept constant between two subsequent time instants contained in $\mathscr{D}$. This means that the input of the controller at time t, is equal to

$$e_{\theta,hyb}(t) := e_{\theta,mea}(t') \text{ with } t' = \max\{\tau \in \mathscr{D} \mid \tau \leqslant t\}. \tag{11}$$

Since the controller output (fixed synchronous update frequency) and its input (asynchronous) are essentially different, this mixed control structure is called 'hybrid'. The PI-controller obtained in Section 3 is not suited for implementation in the hybrid scheme. Indeed, in the synchronous control scheme the choice of the integrative action (given by I) is based on a certain sample period (0.0005 s). In the hybrid scheme, the time between two updates of the error $e_{\theta,hyb}$ will be much larger (especially for low speeds). Hence, implementing the same controller in the hybrid scheme, causes the integrative action to grow too large between slave encoder pulses. To avoid instability the integral constant I of the PI-controller has been decreased by trial and error on the test set-up resulting in a new value $I = 15 \times 10^{-5}$. The pseudo-code for the hybrid control strategy (without feedforward and anti-wind-up) can be found in the appendix.

All the controllers have been implemented and tested with a Digital Signal Processor. To be specific, the real-time control environment from the dSPACE company (Paderborn, Germany) has been used in the prototyping stage. It consists of a processor board (DS1003) equipped with a TMS 320C40 60 MHz DSP and data acquisition hardware. The encoder signals are captured with a digital waveform capture board (DS5001) which is able to trigger on digital events (e.g. the encoder pulses) and store the time stamps with a 25 ns resolution. The DS5001 is equipped with two 32-bit counters. The actuator has been connected to a D/A board (DS2102) with 16 bits resolution and 3 μs settling time. Note that for the implementation in an industrial environment cheap microcontrollers can be used. The obtained experimental results are shown in Fig. 7 for $N = 1$.

If this figure is compared to Fig. 5, where the full encoder resolution is used, it can be seen that the lower encoder resolution does not result in larger position errors using the technique described above. In view of the considerable reduction of resolution (factor 1024), this seems remarkable. The estimated position error $e_{\theta,hyb}$ (see (11)) provides a good estimation of the real position error $e_\theta(t)$ for low frequencies. Since the PI-controller mainly influences low frequencies, the hybrid controller does not display poorer performance. Note that in contrast with the implementation in Section 3 for a low-resolution encoder, the input $e_{\theta,hyb}$ of the controller is equal to zero in case that the real position error e_θ is identically zero.

6. Asynchronous control

In the asynchronous control scheme, presented in this section, both the position error estimate and the control signal will be updated at slave position measurements only (i.e. $t \in \mathscr{D}$). For an asynchronous controller, classical design methods are not applicable, because the control updates are not synchronous in time (i.e. equally spaced on the time axis) and not known a priori. In this section, a new design technique is proposed, based on a transformation of the system into a form that is suitable for the application of the classical control techniques.

6.1. Transformation

Although the measurements and control updates are asynchronous in time, they are equally spaced as a function of the motor position, because the notches (levels) of the encoder have an equidistant distribution along the axis of the slave. The idea is to transform the model description (1) with independent variable time to an equivalent model in which the slave motor position is the independent variable. In the new system representation the measurements will be equidistant in the independent variable.

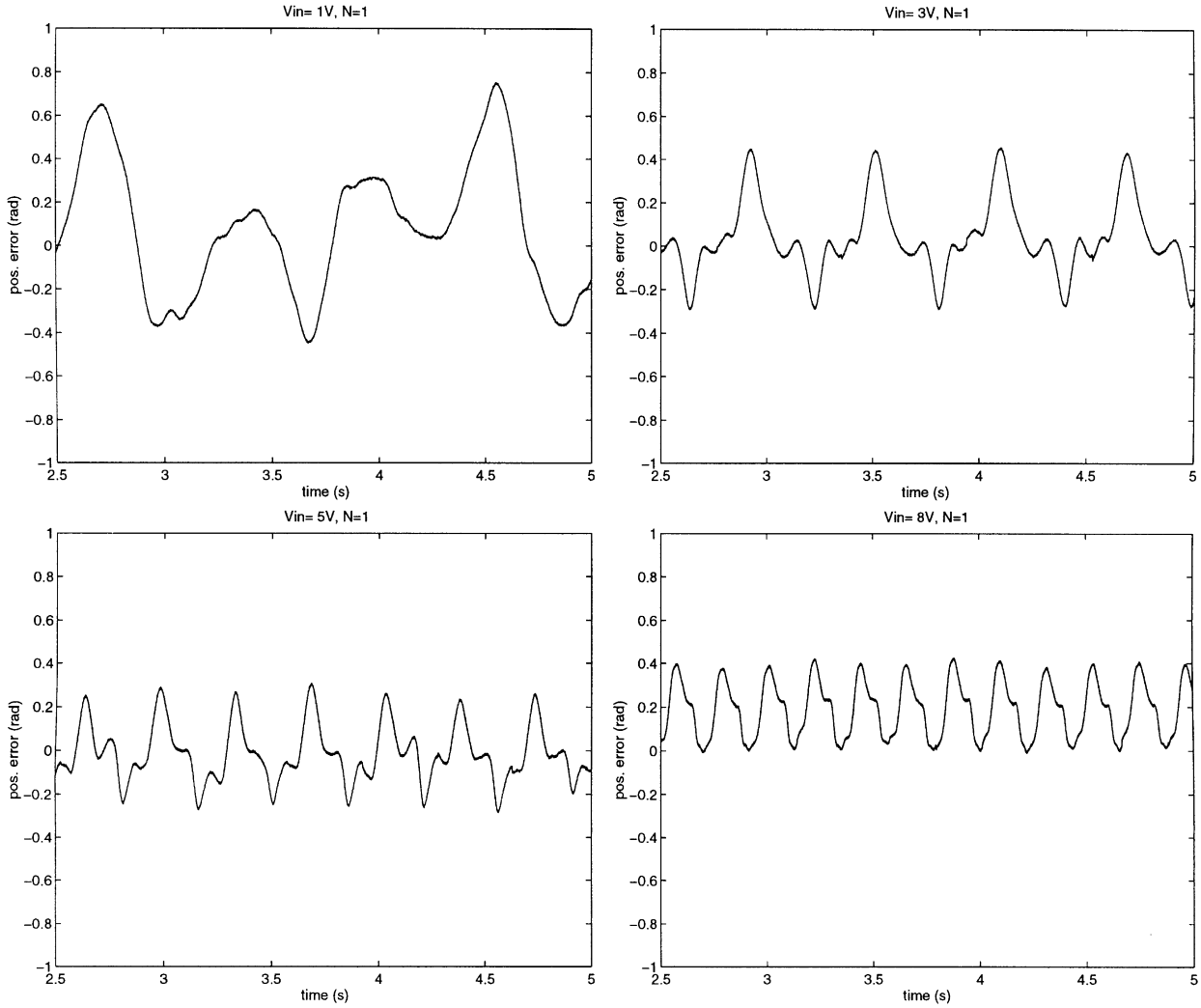

Fig. 7. Real experimental position error with a hybrid controller. The graphs correspond to the same speeds as in Fig. 5. The quantities and scales of the axes are also similar.

The transformation from the time domain (t) to the (slave) position domain (θ_s) can be made by recalling the following relation from (1):

$$\frac{\mathrm{d}\theta_s}{\mathrm{d}t}(t) = \omega_s(t). \tag{12}$$

Now consider θ_s no longer a function of time t, but let time t be a function of the angular position θ_s. The notation $t(\theta_s)$ then denotes the time at which the slave reaches position θ_s. With this interpretation, $\omega_s(\theta_s)$ denotes the angular velocity of the slave motor when the axis is at position θ_s. To simplify notation, θ_s will be replaced by θ, if it does not give rise to confusion.

If $\omega_s(t) \neq 0$, (12) can be rewritten as

$$\frac{\mathrm{d}t}{\mathrm{d}\theta}(\theta) = \frac{1}{\omega_s(\theta)}. \tag{13}$$

Under the assumption that $\omega_s(t) \neq 0$ for all $t > 0$, a one-to-one correspondence between θ and t exists and an interchange of their roles is possible. The interpretation of the requirement $\omega_s(t) \neq 0$ is that the slave motor may not change its direction of movement and must be in its dynamic mode with nonzero velocity all the time. Under normal operating conditions this condition is guaranteed.

Using (13), the system description (1) can be rewritten as

$$\frac{\mathrm{d}t}{\mathrm{d}\theta}(\theta) = \frac{1}{\omega_s(\theta)}, \tag{14a}$$

$$\frac{\mathrm{d}\omega_s}{\mathrm{d}\theta}(\theta) = \frac{1}{J}\left[\frac{T(\theta)}{\omega_s(\theta)} - \frac{d(\theta)}{\omega_s(\theta)} - B\right], \tag{14b}$$

$$\frac{\mathrm{d}T_s}{\mathrm{d}\theta}(\theta) = \frac{1}{\tau}\left[K_t K_f \frac{u(\theta)}{\omega_s(\theta)} - \frac{T(\theta)}{\omega_s(\theta)} - K_t\right], \tag{14c}$$

where $T(\theta)$, $d(\theta)$, $u(\theta)$ denote the torque generated by the slave motor, the disturbance torque and the control value, respectively, when the slave position is equal to θ. The argument of the quantities will indicate whether they are considered as a function of time or (slave) position. Interestingly, time t is now a state of the model. Moreover, the output of the new representation will be the time $t(\theta)$, i.e.

$$y(\theta) = t(\theta). \tag{15}$$

Note that the output is only available when θ is equal to an integer-multiple of δ_s.

The position error between the master and the slave motor axis in the time domain can be related to the time error between the arrival of the master and slave at the same position. The time error $e_t(\theta)$ equals $t_s(\theta) - t_m(\theta)$, where $t_s(\theta)$ and $t_m(\theta)$ denote the time instants at which the slave and master motor axis, respectively, reach position θ. Note that the set $\mathscr{D}$ can be rewritten as

$$\mathscr{D} = \{t_s(j\delta_s) | j \in \mathbb{N}\}. \tag{16}$$

In Fig. 8, a possible position characteristic for the master (θ_m) and slave motor (θ_s) is drawn.

From Fig. 8 it follows that

$$\frac{e_\theta(t_1)}{e_t(\theta_0)} = \omega_r\,, \tag{17}$$

where ω_r is the master motor (reference) speed. This relation is exact when ω_r is constant in the time interval (t_0, t_1). If ω_r is not constant, (17) can be used as an approximation. Since the fluctuations in the load of the conveyor belt (master) are relatively small, the master motor will run at an (almost) constant speed. From (17), it is evident that reducing $e_\theta(t_0)$ is equivalent to reducing $e_t(\theta_0)$. The control objective can thus be reformulated as follows: design a controller H_c in the position domain that maps $e_t(k\delta_s)$, $k \in \mathbb{N}$ (note that the sample interval equals δ_s) to control inputs $u(k\delta_s)$ such that the time error $e_t(\theta)$ satisfies $|e_t(\theta)| \leqslant 1.25/\omega_r$. The requirement on $e_t(\theta)$ follows by combining (3) and (17).

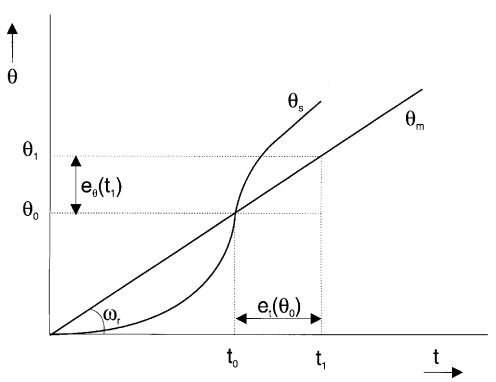

Fig. 8. Master and slave position.

6.2. Design

The transformation of the system description results in a synchronous control problem for a non-linear model (14). As a first approach to the control design for (14), linearization is used around 'equilibrium' trajectories corresponding to a constant master motor speed (normal operating conditions). A steady-state trajectory is

$$(t_0, \omega_0, d_0, T_0, u_0) = \left(\frac{1}{\omega_r}\theta, \omega_r, \bar{d}, B\omega_r + \bar{d}, \frac{1}{K_f}\left[\omega_r + \frac{B\omega_r}{K_t} + \frac{\bar{d}}{K_t}\right]\right), \tag{18}$$

where $\bar{d}$ denotes the mean value of the disturbance d and ω_r the constant master motor speed. The variations around this equilibrium trajectory are denoted by $(\tilde{t}, \tilde{\omega}, \tilde{T}, \tilde{d}, \tilde{u})$. Hence, $t = t_0 + \tilde{t}$, $\omega_s = \omega_0 + \tilde{\omega}$, etc. Around the equilibrium trajectory, the linearized dynamics are

$$\frac{\mathrm{d}\tilde{t}}{\mathrm{d}\theta} = -\frac{1}{\omega_r^2}\tilde{\omega}, \tag{19a}$$

$$\frac{\mathrm{d}\tilde{\omega}}{\mathrm{d}\theta} = \frac{1}{J\omega_r}[-B\tilde{\omega} + \tilde{T} - \tilde{d}\,], \tag{19b}$$

$$\frac{\mathrm{d}\tilde{T}}{\mathrm{d}\theta} = \frac{1}{\tau\omega_r}[-K_t\tilde{\omega} - \tilde{T} + K_t K_f\,\tilde{u}], \tag{19c}$$

$$\tilde{y} = \tilde{t}, \tag{19d}$$

where all signals are functions of θ.

A feedback controller whose output defines the first-order variation $\tilde{u}$ needs to be designed. The controller output $\tilde{u}$ has to be added to the equilibrium value $u_0 = 1/K_f\,(\omega_r + B\omega_r/K_t + \tilde{d}/K_t)$ to generate the control input u. The feedforward signal coming from the master frequency converter takes care of the major part of this constant equilibrium value. The remaining part must be regulated by the feedback controller.

A requirement for the feedback controller is that for all relevant reference speeds ω_r the closed-loop system (of the linearized system) is stable. The interpretation of stability here is that the original system has a zero steady-state error when the master reference speed is ω_r (assuming that the disturbance $\tilde{d}$ is zero). Furthermore, the influence of disturbances must be small and the relative damping of the closed-loop system must be unsensitive for variations in the reference speed ω_r. This yields the same behaviour in the time domain for all reference speeds, as will become clear later.

To proceed, the system description will be discretized in the position domain and a PI-controller

$$H_c(z^*) = K_c\frac{z^* - a}{z^* - 1} \tag{20}$$

will be designed using the root locus method. Note that z^* is used instead of z to emphasize that the discretization

has been made in the position domain. The location of the zero and the gain are chosen as $a = 0.9$ and $K_c = 41$ such that the system shows a desirable and stable behaviour for $\omega_r = 225$ rad/s. This controller is applied to (19) for other reference speeds ω_r to evaluate whether the behaviour of the corresponding closed-loop systems is acceptable.

In Fig. 9 the root loci are plotted for three values of ω_r (from left to right corresponding to ω_r equal to 138, 225 and 362.5 rad/s, respectively, which comply to the input voltages to the master frequency converter 3, 5 and 8 V, respectively). The closed-loop poles corresponding to the gain $K_c = 41$ are denoted by ' + '-marks and labelled by the input voltages. The amount by which the closed-loop poles shift along the locus increases for decreasing values of ω_r. The relative damping of these poles decreases with decreasing ω_r resulting in different closed-loop behaviours. In Fig. 9, also the closed-loop poles are plotted for several intermediate reference speeds ω_r (ranging from 75 to 375 rad/s) with a gain equal to $K_c = 41$ for the controller. For low speeds, the poles are even outside the unit circle resulting in unstable behaviour. Hence, the controller is unacceptable. As the controller gain K_c determines the amount by which the poles shift over the loci,

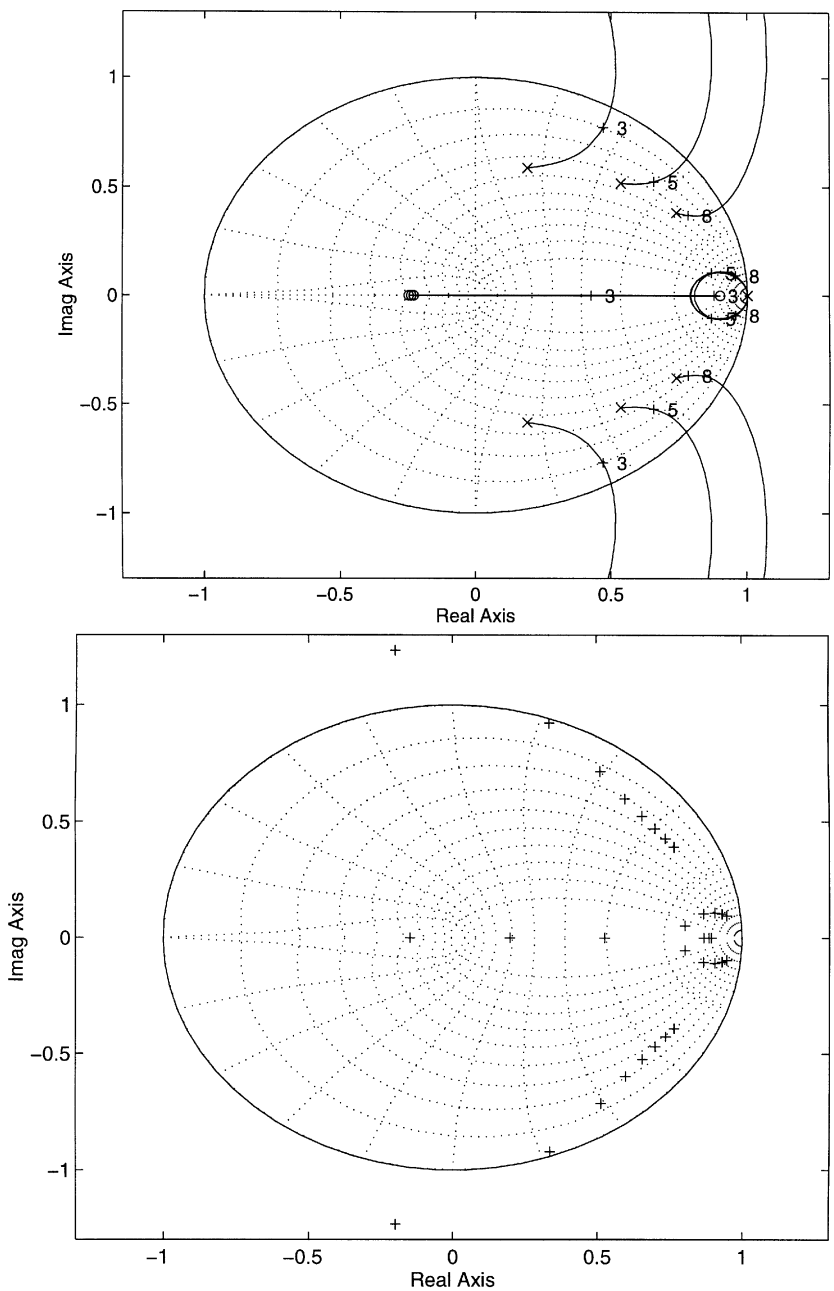

Fig. 9. Root loci (top graph) and pole locations (bottom graph) for varying ω_r and constant controller.

instability of the system can be prevented by choosing a sufficiently small K_c. However, a drawback of low-gain controllers is that some closed-loop poles stay close to the unit circle (slow system). Moreover, the relative damping of the system still depends on ω_r.

One possible solution is to use gain scheduling, i.e. let the controller gain K_c depend on ω_r. From the discussion in the previous paragraph, it is clear that K_c should be smaller for smaller values of ω_r. The gain K_c is therefore chosen to be proportional with ω_r as $K_c(\omega_r) = 0.18\omega_r$ (note that the gain for $\omega_r = 225$ rad/s remains the same as before). Again the root loci are drawn for the same values of ω_r as before (Fig. 10). The ' + ' refers again to the closed-loop poles for $K_c(\omega_r) = 0.18\omega_r$. Note that the relative damping of the complex conjugate poles is almost constant and stability is ensured for all values of ω_r as can be seen from Fig. 10, where the closed-loop poles are drawn for the same values as in Fig. 9.

To show that the closed-loop properties do not depend on the reference value ω_r, step responses are drawn in the upper part of Fig. 11 for ω_r equal to 138, 225, 362.5 rad/s. The interpretation of a unit step here is that the master position (the reference) instantaneously reaches the next

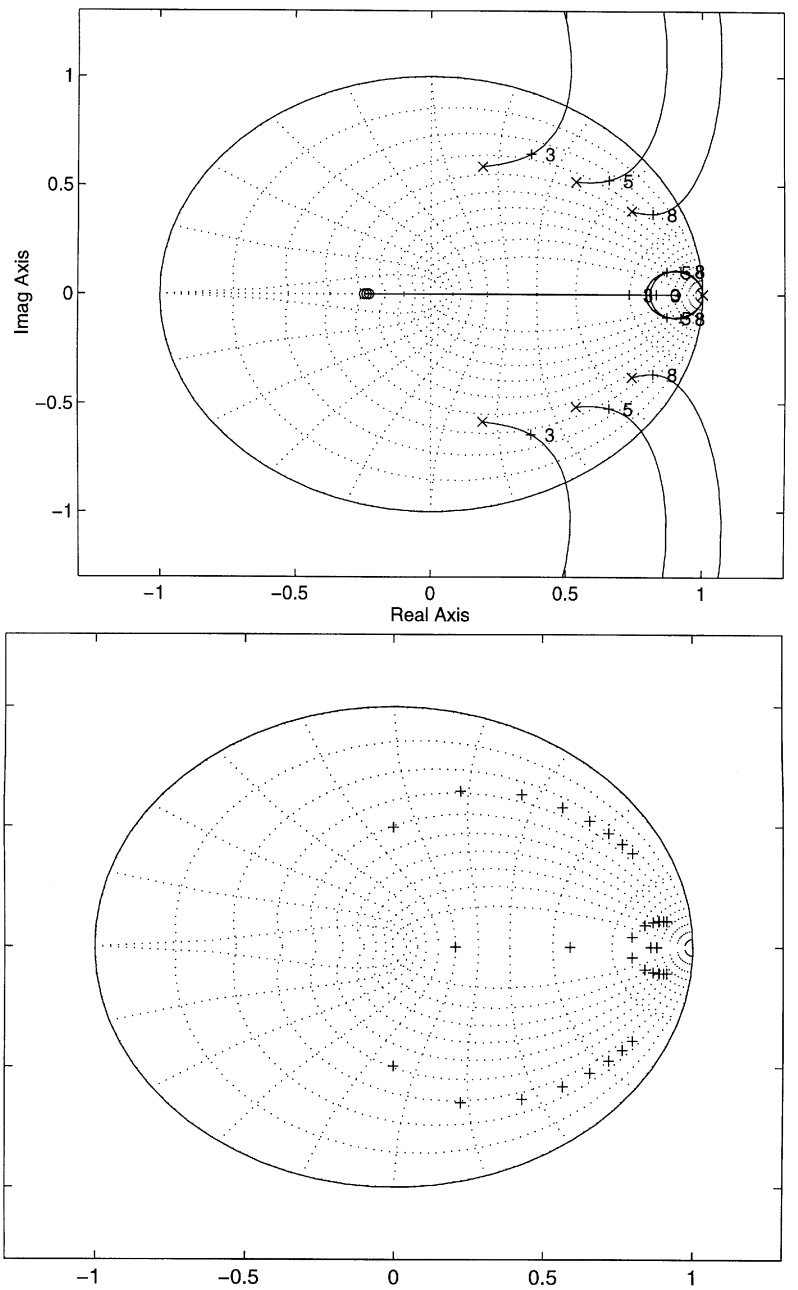

Fig. 10. Root loci (top graph) and pole locations (bottom graph) for varying ω_r and varying controller gains K_c.

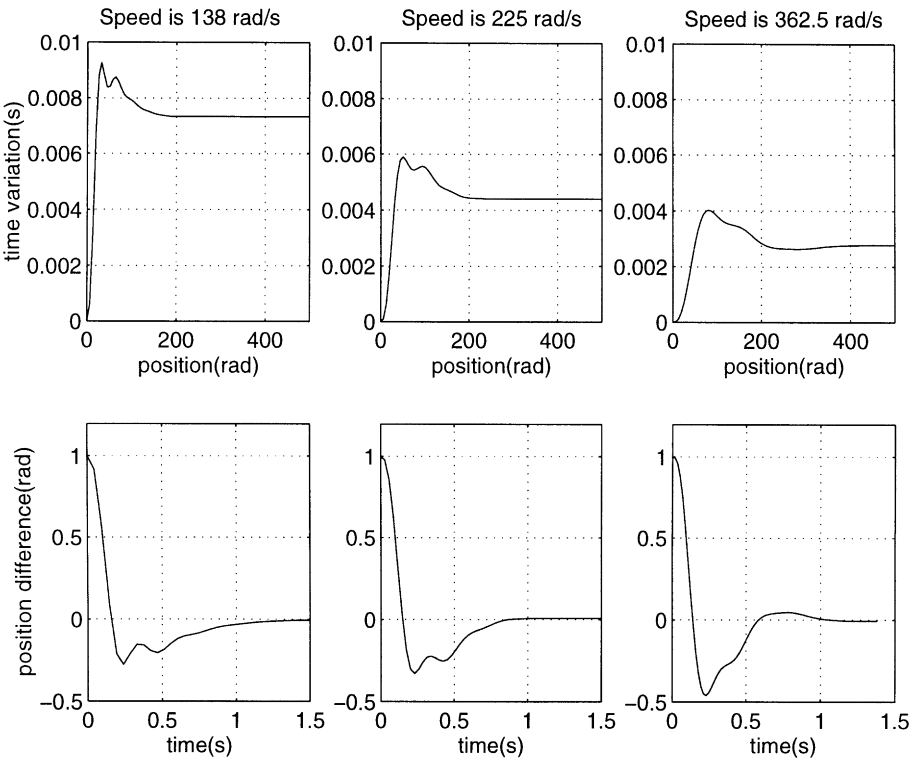

Fig. 11. Step responses of the closed-loop system for varying reference speeds and the transformed position errors.

position exactly one second later. Consequently, the step response displays the time variation (with respect to the equilibrium trajectory $(1/\omega_r)\theta$) at which the slave reaches a certain position. The step heights for different reference speeds are normalized by multiplying with $1/\omega_r$ to get a step of 1 rad on the position error $e_\theta(t)$. In the lower part of Fig. 11, the resulting position errors $e_\theta(t)$ are drawn with respect to time. The position errors stay within the bound of 1.25 rad. Notice also that the settling time is almost equal for all the three cases. This is caused by the fact that for increasing reference speeds, the natural frequency of the closed loop of the linearized transformed system decreases proportionally, while the relative damping stays the same. In the position domain the sampling instants are equally spaced for varying reference speeds (2π apart). In the time domain, the time between measurements is proportional to the inverse of the reference speeds; the higher the reference speed, the smaller the time that the next measurement becomes available. Hence, the effect of decreasing natural frequencies is cancelled by the effect of closer 'sampling instants' in the time domain. As a consequence, the closed-loop systems in the time domain are equally fast. This is the reason why a closed-loop system with the same relative damping for varying speeds was chosen. The small differences in the time responses are caused by the fluctuations in the poles close to one.

6.3. Implementation

An implementation problem arises if the time error $e_t(\theta)$ is used directly as the input of the gain-scheduled controller. If the slave is lagging behind (e.g. $(k-1)\delta_s \leqslant \theta_s(t) < k\delta_s$ and $(l-1)\delta_s \leqslant \theta_m(t) < l\delta_s$ for $l > k$), then all the time instants $t_m(k\delta_s)$, $t_m((k+1)\delta_s), \ldots, t_m((l-1)\delta_s)$ must be stored. Indeed, when the slave reaches the position $j\delta_s$ with $k \leqslant j \leqslant (l-1)$, one needs $t_m(j\delta_s)$ (time of master motor reaching position $j\delta_s$) to determine $e_t(j\delta_s) := t_s(j\delta_s) - t_m(j\delta_s)$. If the slave is ahead of the master the problem is even more serious. The value of $e_t(j\delta_s)$ is not easily retrieved, because the value of $t_m(j\delta_s)$ is not known at time $t_s(j\delta_s)$ (the master motor trajectory is not known a priori). Note that $t_m(j\delta_s) > t_s(j\delta_s)$ and hence, $t_m(j\delta_s)$ is a time instant in the future.

One solution lies in estimating $e_t(j\delta_s)$ by using (17) to convert the position error e_θ (which is known at time $t_s(j\delta_s) \in \mathscr{D}$ with high accuracy) to the time error. This approximation is exact if the reference speed ω_r is constant between $t_s(j\delta_s)$ and $t_m(j\delta_s)$. In view of the (almost) constant master motor speed, the approximation is very accurate, if the actual values of ω_r are known at slave position measurements. Although it seems that a master speed sensor (observer) is needed to determine the actual value of ω_r (master motor speed), this will not be the case as follows from Fig. 12.

Indeed, from Fig. 12, Eq. (20) and the varying gain $K_c(\omega_r) = 0.18\omega_r$, it follows that the factor ω_r in the gain-scheduled controller cancels out the $1/\omega_r$ multiplication needed to convert the position error to the time error. Consequently, the implementation does not depend on ω_r and is of an extremely simple form. Recall the definition of $\mathscr{D}$ as the set of times at which the slave encoder gives a pulse (see (9) and (16)) and denote $t_s(j\delta_s)$ by $t_j, j \in \mathbb{N}$ for shortness. The control value $\tilde{u}$ (see (19)) has to be updated at time t_j according to

$$\tilde{u}(t_j) = \tilde{u}(t_{j-1}) + 0.18e_{\theta,mea}(t_j) - 0.16e_{\theta,mea}(t_{j-1}). \quad (21)$$

The resulting pseudo-code (without feedforward and anti wind-up) is given in the appendix. The feedforward term (see Fig. 2) has to be added to $\tilde{u}$ to obtain the control input u.

The main computational steps can be summarized as follows.

(i) The model for the slave motor (1) is transformed to the position domain by multiplying the right-hand sides by $1/\omega_s$.
(ii) The obtained description (14) is linearized along 'equilibrium trajectories' corresponding to constant master motor speeds.

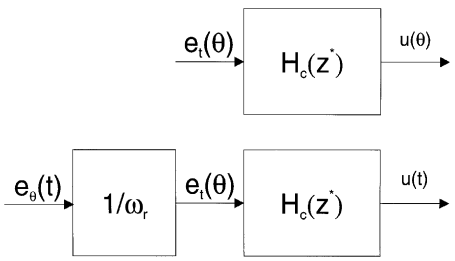

Fig. 12. Top graph: analysed controller, bottom graph: actual implementation.

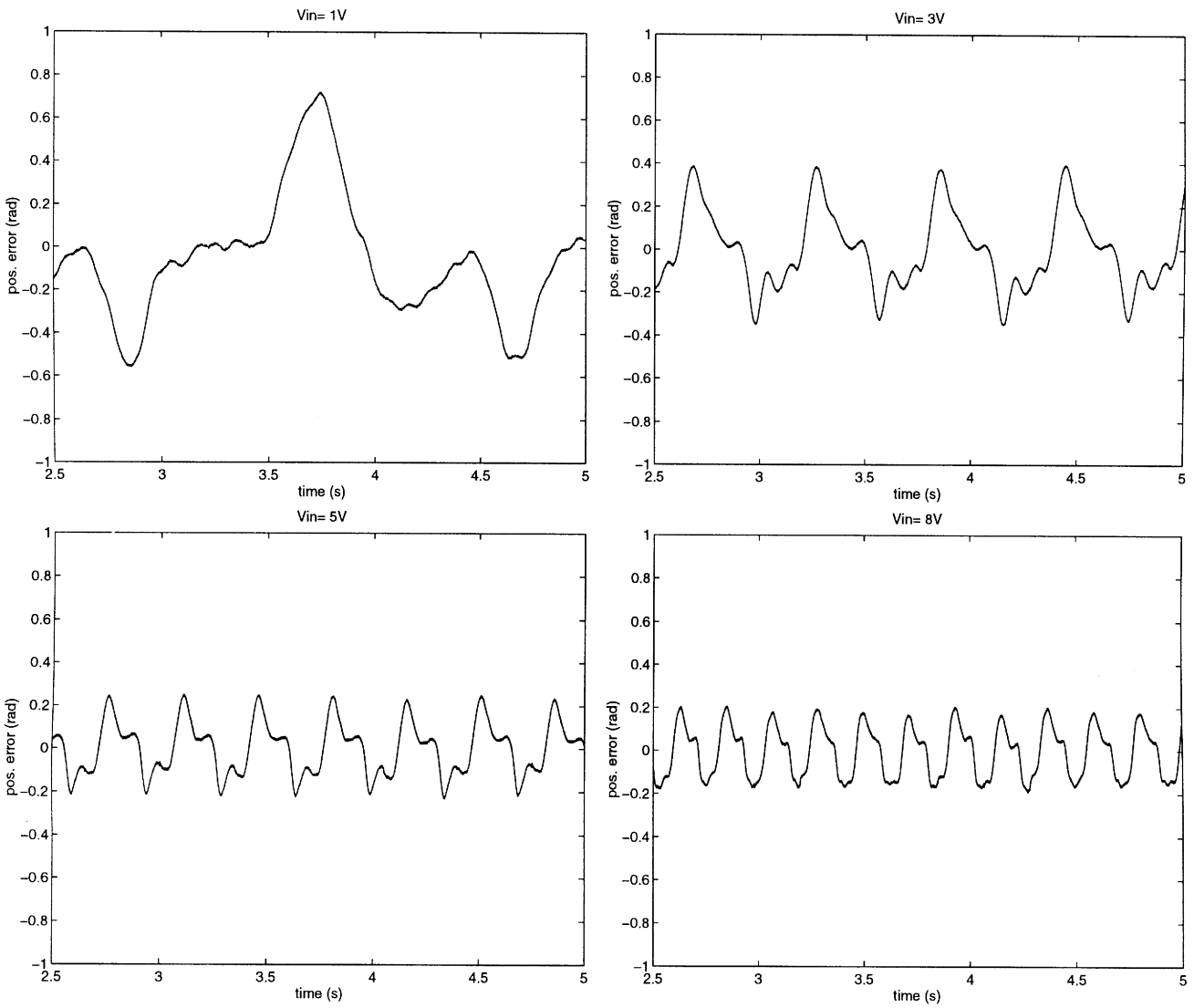

Fig. 13. Position error for asynchronous control using 1 pulse per revolution. The graphs correspond to the same speeds and scales as in Fig. 5.

(iii) Design a PI-controller for one specific linearization ($\omega_r = 225$ rad/s in our case) so that the closed loop is stable and has a sufficiently small relative damping.
(iv) Take a linear varying gain K_c so that the gain remains the same for the specific linearization chosen in the previous step (resulted in $K_c = 0.18\omega_r$).
(v) Since the ω_r-dependence cancels out in the time domain, the feedback controller is implemented as given by (21) and the pseudo-code in the appendix.

6.4. Validation

The designed asynchronous controller has been experimentally validated on the test set-up (Fig. 13). For the reference speeds 42.5, 138, 225 and 362.5 rad/s the position errors are plotted. Observe that the maximum allowable error of 1.25 rad is not exceeded and that the mean of the error is equal to zero. Hence, the designed controller satisfies the required specifications.

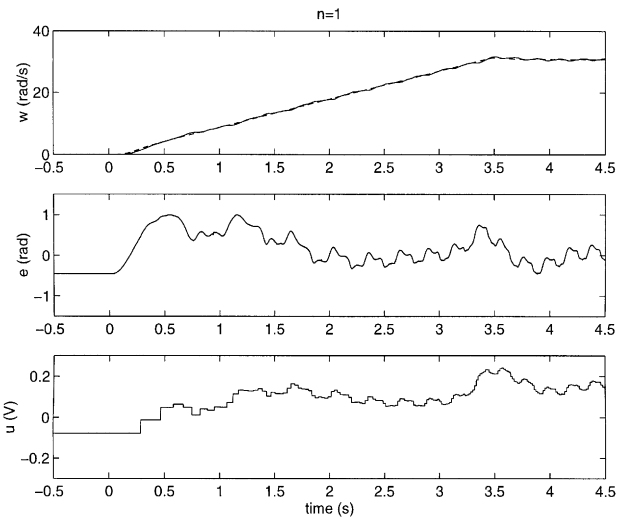

Fig. 15. Starting up the mailing system with asynchronous controller using 1 pulse per revolution.

7. Practically relevant test

Starting up the mailing system is done on a daily basis. At start-up, the master motor speed increases from 0 to 371 rad/s. Due to the gear ratio the load axis speed increases to 29.6 rad/s corresponding to the normal operation speed of the mailing system of 17 000 (!) products per hour.

In Figs. 14 and 15 the results of the hybrid and asynchronous controller are given for 1 pulse per revolution of the slave motor axis. The top graphs display the speed trajectories for both the master (dotted) and the slave load axes (solid) with one measurement per revolution of the motor axis. The graphs in the center show the position errors between master and slave on the motor axis and the lower graphs show the control values of the feedback controller in Volts. One observes that the mailing system can be brought to normal operating conditions in 4.5 s within the required position error bounds. Both developed controllers perform satisfactory.

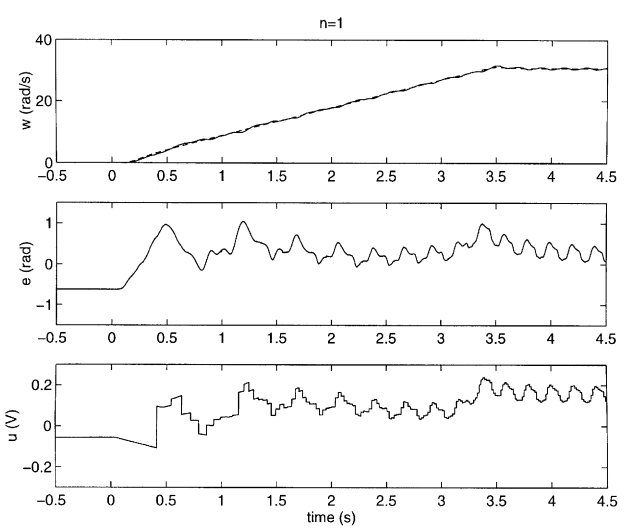

Fig. 14. Starting up the mailing system with hybrid controller using 1 pulse per revolution.

8. Conclusions

The design of controllers for synchronization of a master and slave motor in a mailing system has been studied. To reduce the manufacturing costs of a mailing system, the resolution of the encoder should be low and the control structure simple.

Two control schemes, the hybrid and the asynchronous scheme have been developed and implemented. The main idea has been to use the position error measurements only when the low-resolution encoder provides exact information on the slave position. The accuracy of the measured error is then equal to the accuracy of the high-resolution master motor encoder. The hybrid controller uses only the position error at slave measurements and has a high fixed control rate. For the test set-up a resolution of one measurement per revolution suffices. As the controller is a simple first-order system, it is easy to implement. The measurement error, however should be updated asynchronously in time. This calls for some interrupt-driven logic circuits in combination with a fixed timer to generate the output of the controller at fixed time intervals.

In the asynchronous control scheme both the measurement and control updates are not equidistant in time. Both updates are triggered by the slave position

measurement. A new design method is proposed based on transforming the asynchronous linear representation in the time domain into a synchronous nonlinear model in the position domain. A gain-scheduled controller has been developed that resulted in a very simple control structure. It has been shown that sufficient performance can be achieved for resolutions as low as one measurement per revolution. In this case, the implementation requires interrupt-driven logic circuits only.

Both the hybrid and the asynchronous controller meet the required performance for very low encoder resolutions and low costs. The choice between the asynchronous and the hybrid controller largely depends on the ease and costs of the implementations for the specific machine at hand.

A final issue that is worth mentioning, is that for industrial implementation of either the hybrid or asynchronous control scheme, one has to take care that the slave motor keeps on running. Indeed, if the slave motor halts, the slave encoder does not provide new position measurements and the measured position error will not be updated. Such a situation must be prevented by incorporating a stall detector and additional code to the supervisory controller.

In this paper some ideas for control based on asynchronous measurements have been presented. Further research will be concerned with gaining more insight in the process of asynchronous measurements and improving the proposed control strategies.

Acknowledgements

The authors are grateful to the anonymous reviewers for their useful suggestions which helped to improve the overall quality of the paper.

Appendix A. Pseudo-code

In the appendix the pseudo-code (without the feedforward of the signal coming from the master frequency converter and the anti wind-up techniques) for the various control structures is presented. The following comments are needed to understand the code.

- The commands **if** are triggered by the encoder of master or slave (hardware of the system) or the timer reaching the next update.
- All the **if**-statements run in parallel.
- 'UpdateError()' reads out the master and slave counters and computes the position error.
- The command 'UpdateController()' recomputes the control value based on the available position error.

A.1. Synchronous controller

```
while TRUE do,
    if SlavePulse,
        IncrementSlaveCounter()
    end
    if MasterPulse,
        IncrementMasterCounter()
    end
    if TimePulse,
        UpdateError();
        UpdateController()
    end
end
```

A.2. Hybrid controller

```
while TRUE do,
    if SlavePulse,
        IncrementSlaveCounter();
        UpdateError()
    end
    if MasterPulse,
        IncrementMasterCounter()
    end
    if TimePulse,
        UpdateController()
    end
end
```

A.3. Asynchronous controller

```
while TRUE do,
    if SlavePulse,
        IncrementSlaveCounter();
        UpdateError();
        UpdateController()
    end
    if MasterPulse,
        IncrementMasterCounter()
    end
end
```

References

Bamieh, B. A., & Pearson Jr., J. B. (1992). A general framework for linear periodic systems with applications to H_∞ sampled-data control. *IEEE Transactions on Automatic Control*, *37*(4), 418–435.

Bruin, D. de, & van den Bosch, P.P.J. (1998). Measurement of the lateral vehicle position with permanent magnets. *Proceedings of the IFAC workshop on intelligent components for vehicles (ICV'98)*, Seville, Spain (pp. 9–14).

Chen, T., & Qiu, L. (1994). H_∞ design of general multirate sampled-data control systems. *Automatica*, *30*, 1139–1152.

Chiang, W.-W. (1990). Multirate state space digital controller for sector servo systems. *Proceedings of the 29th conference on decision and control*, Honolulu, Hawaii (pp. 1902–1907).

Franklin, G.F., Powell, J.D., & Naeni, A.E. (1994). *Feedback control of dynamic systems*. Amsterdam: Addison-Wesley.

Gorter, R.J. (1997). *Grey-box identification of induction machines*. Ph.D. thesis, Dept. of Electrical Engineering, Eindhoven University of Technology, The Netherlands.

Hori, Y., Umeno, T., Uchida, T., & Konno, Y. (1991). An instantaneous speed observer for high performance control of DC servo-motor using DSP and low precision shaft encoder. *Proceedings of Fourth European conference on power electronics and applications*, Firenze, Italy (pp. 647–652).

Leonhard, W. (1990). *Control of electrical drives*. (pp. 204–237) Berlin: Springer.

Peng, Y., Vrancic, D., & Hanus, R. (1996). Anti-windup, bumpless and conditioned transfer techniques for PID controllers. *IEEE Control Systems Magazine*, *16*(4), 48–57.

Phillips, A.M., & Tomizuka, M. (1995). Multirate estimation and control under time-varying data sampling with applications to information storage devices. *Proceedings of the 1995 American control conference*, (pp. 4151–4155) vol. 6, American Autom. Control Council, Evanston, Illinois.

Sågfors, M. F., & Toivonen, H. T. (1997). H_∞ and LQG control of asynchronous sampled-data systems. *Automatica*, *33*(9), 1663–1668.

Voulgaris, P. G. (1994). Control of asynchronous sampled-data systems. *IEEE Transactions on Automatic Control*, *39*(7), 1451–1455.

Zijl, A. van (1997). *Asynchronous motor control*. Master of Science thesis, Dept. of Electrical Engineering, Eindhoven University of Technology, The Netherlands.